Supplementary Information Available

Experimental Section

Homology model

The 3D structure of hAQP3 was obtained by homology modelling using the Molecular Operating Environment (MOE 2013.08)[1]. The choice of a template structure was based on the sequence identity between hAQP3 and the sequence of the AQPs with available resolved structures. The isoform showing the highest sequence similarity with hAQP3 is the bacterial isoform GlpF, with 34.68% of sequence identity, which was then chosen as a template structure to generate a homology model of hAQP3. The template was selected among the structures with the best resolution (2.2 Å, pdb 1FX8).[2] The homology model was prepared and refined as described in[3–5].

Metadynamics was chosen to study the free energy and mechanism of H_2O_2 conductance. A second method, transition path sampling (TPS), was used to calculate unbiased trajectories of H_2O_2 permeation and gain a higher resolution insight into the interactions during a conductance event. Each simulation box contained the AQP3 tetramer homology model inserted into a lipid bilayer, made up of 166 POPC lipids (carried out using the charm GUI online server[6,7]). Each system was solvated with ca. 33000 TIP3P water molecules. Four Na^+ ions were substituted for corresponding water molecules to neutralise the charges of each system. Periodic boundary conditions (PBC) were used for each system.

Metadynamics simulations

Well-tempered metadynamics simulations were run for 200,000,000 steps with a 1 fs time-step (200 ns) using the Plumed plugin[8] for Gromacs. The distance collective variable (CV) was used between the COM of H_2O_2 molecules and a plane formed by the backbone carbons of Asparagine 215 from each of the four monomers. This provided a reference plane in the centre of the system, equating to the top of the NPA motif. Each of the 20 H_2O_2 molecules were given a separate plumed control within the same data file, allowing the free-energy for each molecule to be calculated within the same simulation. Gaussians were added every 100 steps (0.1 ps), giving a deposition rate of 1.25 kJ/mol.ps. Gaussian height was 0.0125 kJ/mol and the Gaussian width was 0.0625 Å. The bias factor was set to 12, ΔT was 3600 K.

Free energy surface data were normalised by setting the baseline to 0 and excluding bulk water on either side of the pore to show more clearly the data for each permeation event. The individual FES plots for H_2O_2 were taken from the trajectories in which a H_2O_2 passed through a pore, in either direction, once during the simulation. Data for any H_2O_2 molecules re-crossing the pore or passing through the lipid membrane were not included. This resulted in 22 FES of H_2O_2 passage (12 for uptake and 10 for efflux), which were used for calculating ΔG values.

The amber99sb-ildn+slipid force field was used for all simulations, with the parameters for H_2O_2 generated by the Automated Topology Builder and Repository (ATb, version 2.2) website using the B3LYP/6-31G* basis set [9], using a combination of semi-empirical quantum mechanics (QM) and density functional theory (DFT). All simulations were run using the GROMACS 2016.3 software[10]. Particle-mesh Ewald method was used for calculating long-range electrostatic interactions, the Verlet cut-off scheme with a cut-off distance of 0.7 nm was used for short range repulsive and attractive interactions and Lincs was used to constrain all bond lengths. Nose-hoover[11] temperature coupling was used to maintain the temperature of the system (τ = 0.5 ps) at 300 K. The Parrinello-Rahman[12] algorithm was used to maintain the pressure of the system at 1 bar with a coupling constant of τ = 1.0 ps. Simulations were equilibrated for 100 ps before production. Total energy of the system was monitored using gmx_energy program within Gromacs until total energy changes were less than 0.4% over 75 ps (Figure S4).

Transition Path Sampling (TPS)

TPS requires the generation of a first trajectory. This was obtained from configurations along metadynamics trajectories. A single H_2O_2 molecule positioned between the ar/R and NPA motifs of an AQP3 monomer was used for the starting positions of the TPS calculations. The system and conditions matched those used for the metadynamics simulations as well as the order parameter used to decide on the success of a trajectory. A timestep of 1fs was used with individual calculations running for either 500 ps, 1ns or 2 ns depending on the progress of the H_2O_2 along the trajectory. Once the molecule moved away from the starting position, in either direction along the *z* axis, the timestep was reversed. This was continued until multiple occurrences of the H_2O_2 molecule had moved from the NPA to the bulk solvent. Multiple trajectories were then combined to produced full conductance events from the extracellular to the cytoplasmic side of the AQP3 monomer.

Movies

Movie **M1.** Metadynamics calculated trajectory of H_2O_2 conductance. A single H_2O_2 is shown traversing the pore. Selected waters have been coloured based on their initial positions to highlight the bidirectional 'hopping' mechanism. Green = initially positioned in the channel, purple = originate from the extracellular side, pink = originate from the cytoplasmic side.

Movie **M2.** TPS calculated trajectory of H_2O_2 conductance. A single H_2O_2 is shown traversing the pore. One oxygen atom of H_2O_2 is coloured yellow to provide a clear indication of orientation changes. Selected waters have been coloured based on their initial positions to highlight the bidirectional 'hopping' mechanism. Green = initially positioned in the channel.

Movie **M3**. TPS calculated trajectory of H_2O conductance. A single H_2O, coloured blue, is shown traversing the pore. Selected waters have been coloured based on their initial positions to highlight the bidirectional 'hopping' mechanism. Green = initially positioned in the channel. Water hydrogen bonds are shown in dashed red to indicate the H-bond chain.

Figures

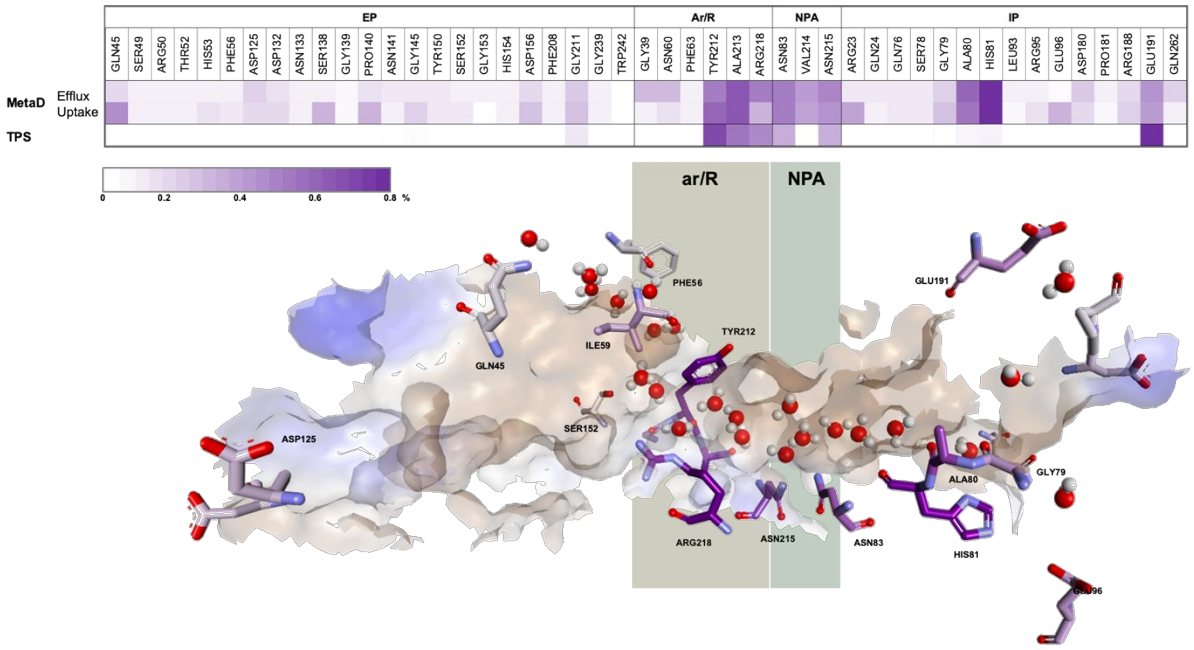

Figure S1. H_2O permeation routes and H-bond patterns and RT (%) from metadynamics and TPS calculations. Average H-bond RT (%) of H_2O during uptake and efflux (on a scale of 0-0.8%) shown in a gradient purple colour, with the strongest colour indicating the highest RT. Multiple H_2O molecules snapshots, taken from one representative simulation, are overlaid in one structure to create one single path. Amino acids that form crucial H-bonds are explicitly shown. Carbons are colour-mapped (white to purple) according to their corresponding RT (short to long). Pore colour representation based on hydrophobicity of the pore surface, blue = hydrophilic, brown = hydrophobic. Picture adapted from Wragg et al, *Chemistry Eur J.*, 2017.

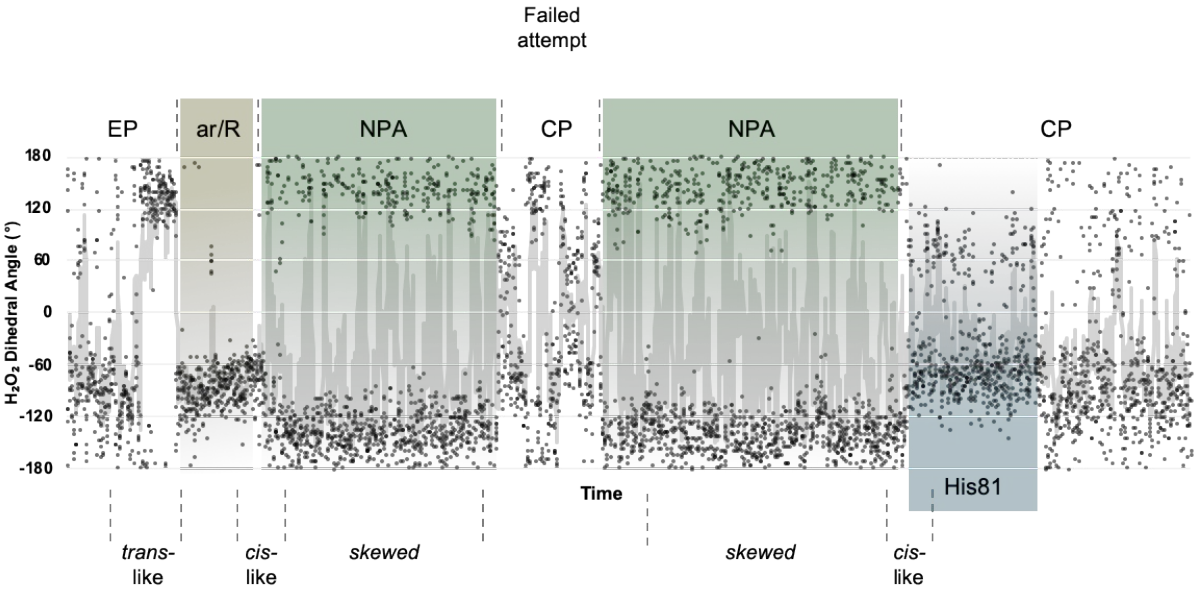

Figure S2. Plot charting the H_2O_2 dihedral angle change throughout a conductance event. Key pore motifs, coloured yellow for the ar/R SF and green for the NPA indicate when H_2O_2 passes through these regions, along with the average conformation based on the dihedral angle. A failed attempt to exit the pore is indicated, whereby H_2O_2 then re-enters the NPA motif. Interactions with the highly conserved His81, located in the cytoplasmic pocket (CP) are indicated in blue. The overlaid grey line graph indicates the moving average trendline of the dihedral angle every ten frames throughout the trajectory.

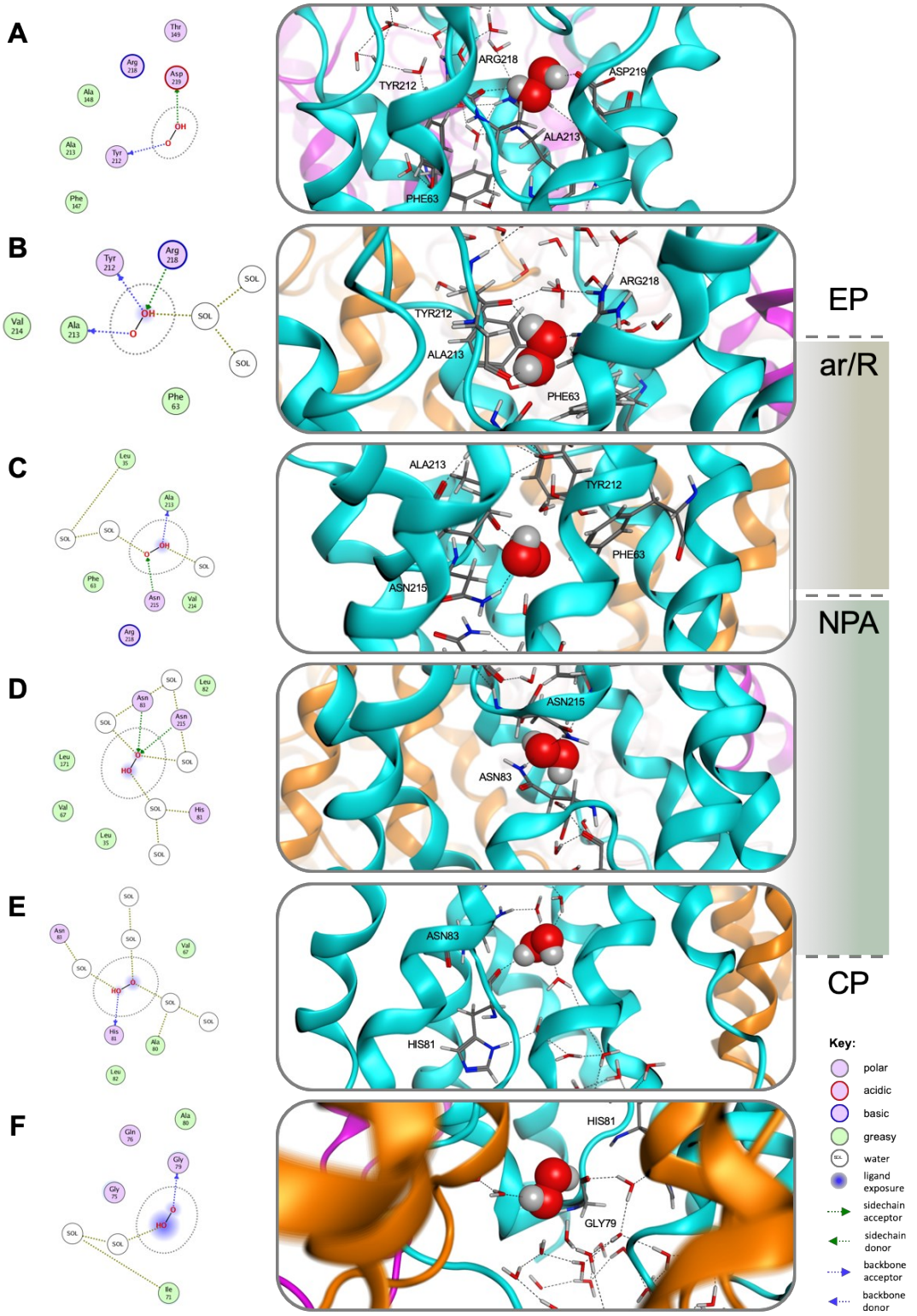

Figure S3. A-F, Position, orientation and H-bond interaction of H_2O_2 during conductance through the hAQP3 monomer form the extracellular pocket (EP) to the cytoplasmic pocket (CP). Figure generated using Molecular Operating Environment MOE software[13].

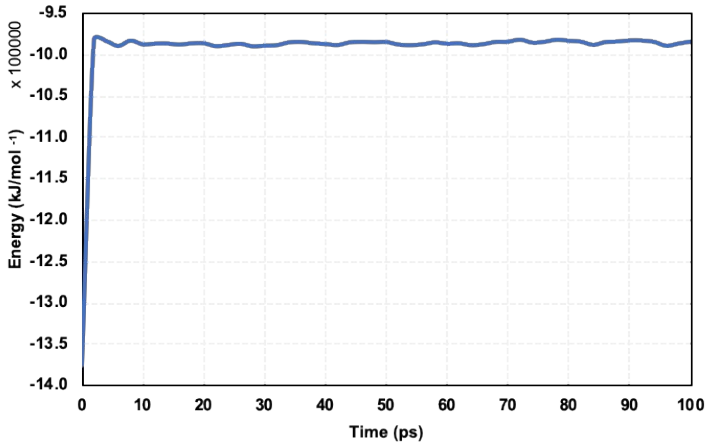

Figure S4. Total energy during 100 ps equilibration step for AQP3 with H_2O_2.

References

[1] C. C. Group, "Molecular Operating Environment (MOE 2010).," can be found under http://www.chemcomp.com, **2010**.

[2] D. Fu, A. Libson, L. J. W. Miercke, C. Weitzman, P. Nollert, J. Krucinski, R. M. Stroud, *Science (80-.).* **2000**, *290*, 481–486.

[3] A. Spinello, A. De Almeida, A. Casini, G. Barone, *J. Inorg. Biochem.* **2016**, *160*, 78–84.

[4] A. De Almeida, A. P. Martins, A. F. Mósca, H. J. Wijma, C. Prista, G. Soveral, A. Casini, *Mol. Biosyst.* **2016**, *12*, 1564–1573.

[5] A. De Almeida, A. F. Mó, D. Wragg, M. Wenzel, P. Kavanagh, G. Barone, S. Leoni, G. Soveral, A. Casini, *Chem. Commun.* **2017**, 3830–3833.

[6] S. Jo, T. Kim, V. G. Iyer, W. Im, *J. Comput. Chem.* **2008**, *29*, 1859–1865.

[7] E. L. Wu, X. Cheng, S. Jo, H. Rui, K. C. Song, E. M. Dávila-Contreras, Y. Qi, J. Lee, V. Monje-Galvan, R. M. Venable, et al., *J. Comput. Chem.* **2014**, *35*, 1997–2004.

[8] G. A. Tribello, M. Bonomi, D. Branduardi, C. Camilloni, G. Bussi, *Comput. Phys. Commun.* **2014**, *185*, 604–613.

[9] A. K. Malde, L. Zuo, M. Breeze, M. Stroet, D. Poger, P. C. Nair, C. Oostenbrink, A. E. Mark, *J. Chem. Theory Comput.* **2011**, *7*, 4026–4037.

[10] M. J. Abraham, T. Murtola, R. Schulz, S. Páll, J. C. Smith, B. Hess, E. Lindah, *SoftwareX* **2015**, *1–2*, 19–25.

[11] S. Nosé, *Mol. Phys.* **1984**, *52*, 255–268.

[12] M. Parrinello, A. Rahman, *Phys. Rev. Lett.* **1980**, *45*, 1196–1199.

[13] C.C. Group, **2018**.